 DOI: 10.19601/j.cnki.issn1943 – 9903.2026.07.005

Superposition of a Warm-Sector Rainstorm and Train Effect: Characteristics and Early Warning Difficulties of an Extreme Rainstorm in Sanming City in June 2024

Yijie YANG[1,2], Pengyu WU[3], Shuqi DENG[1], Xiaodong GUAN[1]

1. Sanming Meteorological Bureau, Sanming 365000, China; 2. Fujian Key Laboratory of Disaster Weather, Fuzhou 350001, China; 3. Shaxian Meteorological Bureau, Sanming 365500, China

Abstract Based on the data of conventional radiosonde observations, the new generation Doppler radar, FY-4B satellite, regional assimilation products, *etc.*, a regional extreme rainstorm in Sanming City from 20:00 on June 12 to 20:00 on June 13, 2024 was analyzed from the aspects of weather conditions, circulation patterns, mesoscale evolution, and numerical model deviations. Through a horizontal comparison among the towns in Nanping, Sanming, and Longyan that experienced heavy precipitation during this process, as well as a vertical comparison with the rainstorm in Taining on May 8, 2016, the difficulties and indicators for forecasting warm-sector rainstorms in this region were summarized to provide a reference for the forecasting and warning of similar extreme warm-sector rainstorms in northwestern Fujian. The results show that the regional extreme rainstorm in Sanming City from 20:00 on June 12 to 20:00 on June 13, 2024 was characterized by concentrated precipitation and extreme short-term rainfall intensity. The cumulative rainfall in Xiaqu Town, Taining County was 264.7 mm, and the hourly rainfall intensity in Bailian Town, Jiangle County was 81.3 mm. Due to the combined influence of the southwest jet stream, low-level shear, and deep warm moist air flow, the superposition of a warm-sector rainstorm and train effect was the core cause of the disaster.

Key words Extreme rainstorms, Warm-sector rainstorms, Train effect

0 Introduction

In the pre-flood season (from April to June) in South China, warm-sector rainstorms appear frequently. In Fujian, which is located in the east of South China, warm-sector rainstorms in the pre-flood season are characterized by strong suddenness, large short-term rainfall, and prominent local features under the influence of south troughs, high- and low-level jet streams, complex mountainous terrain, and sea and land moisture transport. Their forecast has always been a difficult point in short-term forecast. In the northwest of Fujian, under the coupling effect of the southwest jet stream, low-level shear, and other systems, continuous extreme heavy precipitation is likely to happen, and train-effect warm-sector rainstorms frequently occur. In history, there have been many regional extreme rainstorms.

At present, domestic meteorological scholars have conducted extensive research on warm-sector rainstorms in Fujian and South China[1–5]. Previous studies mostly focus on a single isolated rainstorm or climate statistical laws, but there are few studies on continuous heavy precipitation processes and detailed and precise reviews of extreme peak periods.

From June 8 to 18, 2024, Sanming City experienced continuous regional heavy rainfall. From 20:00 on June 12 to 20:00 on June 13, there was a regional extreme rainstorm. In Taining, Jiulian, and other areas, 24-hour cumulative rainfall exceeded the historical peak, and short-term rainfall intensity was extremely prominent. The process was mainly dominated by warm-sector rainstorms, which were combined with the echo train effect and the amplification effect of the Wuyi Mountain. In this paper, based on the multi-source data of conventional radiosonde observations, the new generation Doppler radar, FY-4B satellite, regional assimilation products, *etc.*, the precipitation process was analyzed from the aspects of weather conditions, circulation patterns, mesoscale evolution, and numerical model deviations. The environmental field indicators, radar identification characteristics, and forecast shortcomings of the continuous warm-sector rainstorm in northwestern Fujian were summarized, and the focus of the rainstorm forecast and the optimization plan for the warning system were discussed to provide a reference for the forecasting and early warning of similar extreme rainstorms in the pre-flood season in northwestern Fujian.

1 Weather conditions and disaster situation

1.1 Precipitation characteristics From 20:00 on June 12 to 20:00 on June 13, 2024, a historically rare extreme rainstorm occurred in Sanming City. The heavy precipitation was concentrated in Taining, Jiangle, Jianning, and Qingliu in the north of Sanming. The single-station rainfall, hourly rainfall intensity, and 3-hour rainfall intensity during the continuous heavy precipitation process from June 8 to 18 in the city were the strongest during the period. The comprehensive intensity ranked among the top in history since 1961, and it was significantly stronger than the rainstorm on May 8 in 2016.

Cumulative rainfall: the rainfall was ≥50 mm in 82 townships and ≥100 mm in 41 townships across the city; the maximum cumulative rainfall occurred in Xiaqu Town, Taining (up to 264.7

Received: May 5, 2026 Accepted: June 10, 2026
Supported by the Youth Science and Technology Special Project of Fujian Meteorological Bureau (2024Q10).

mm), followed by Kaishan Township, Taining (257.2 mm), and Meikou Township, Tai Ning (233.3 mm); the maximum rainfall in the urban area appeared in Taining, reaching 169.6 mm.

Short-term rainfall intensity: the maximum 1-hour rainfall intensity appeared in Bailian Town, Jiangle County (81.3 mm), and the maximum 3-hour rainfall intensity occurred in Kaishan Township, Taining County (178.8 mm); from 09:00 to 11:00, the continuous 3-hour rainfall intensity in Kaishan Township, Meikou Township, and Xiaqu Town exceeded 40 mm. The short-term rainfall was very extreme.

Main characteristics of the process: firstly, it had significant strong convection and was accompanied by strong convection weather such as short-term heavy precipitation, thunderstorms, and gales; secondly, the duration was long, and heavy precipitation lasted for more than 6 h; thirdly, the precipitation was highly concentrated, and the rain belt was stable and less mobile, forming a distinct train effect; fourthly, it had obvious local characteristics, with a large spatial gradient of the rainstorm center and extremely strong single-point possibility of causing a disaster.

1.2 Disaster situation and its impact During the initial stage of this extreme rainstorm, the entire city had already experienced continuous precipitation, resulting in extremely saturated soil moisture, so this extreme short-term heavy precipitation led to flash floods, rapid rises in the water level of small and medium-sized rivers, urban and rural flooding, landslides, road collapses, inundation of farmland, as well as damage to water conservancy, power, and communication facilities. The heavy rainfall mainly caused geological disasters and urban and rural flooding hazards in Taining, Jiangle, and Qingliu. Thanks to the early release of meteorological warnings, the rapid response of the flood prevention department, timely evacuation calls during the disaster, and the early relocation of the population, this process did not cause significant casualties, during which the life-saving role of meteorological forecasting and warning was fully demonstrated.

2 Analysis of the weather process

2.1 Circulation background and influencing systems This extreme rainstorm process was the result of extreme intensification of the continuous heavy precipitation from June 8 to 18. The circulation background was stable, and the configuration of middle- and lower-level systems was conducive to the continuous development of the heavy precipitation.

500 hPa situation: Fujian Province was under the control of the southwest airflow in front of the trough, and the southern vortex shear system in the Yangtze River Basin developed. The north of Sanming City was located on the south side of the shear, and the 16 m/s southwest jet stream and wind speed convergence superimposed to form a strong dynamic lifting condition, providing stable circulation support for the continuous development of the convection.

Middle- and lower-level conditions: at 850 hPa, specific humidity was 15 – 16 g/kg, and precipitable water vapor (PWV) was 60 – 65 mm, with a deep moisture layer, high dew point temperature, abundant water vapor transport, and obvious convergence; K index was 38 – 40 ℃, and convective unstable energy was sufficient, which was conducive to the occurrence and development of strong convection; in terms of dynamics; there was triple configuration of shear line, southwest jet stream, and wind speed convergence, and vertical ascending motion was strong, continuously triggering and maintaining heavy precipitation. The mesoscale weather chart at 05:00 on June 13, 2024 is shown in Fig.1.

2.2 Diagnosis of physical quantities The sounding data of Shaowu at 08:00 on June 13 show that the north of Sanming had characteristics of the environment field of typical warm-sector rainstorms: convective available potential energy (CAPE) was moderate, and lifting condensation level (LCL) was low, only 372 m, which was conducive to the development of warm cloud precipitation; there was a deep moisture layer and a thick warm cloud layer, so precipitation efficiency was high; K index reached 40 ℃, and convective potential was extremely strong; the configuration in the 0, –10, and –20 ℃ layers was conducive to the occurrence of short-term heavy precipitation, and wet convection was dominant, so hail and thunderstorm gales were unlikely to occur.

2.3 Mesoscale monitoring characteristics

2.3.1 Radar echo characteristics. From 07:00 to 11:00, the northern part of Sanming was continuously affected by strong echoes (Fig.2). After entering Taijin, the echoes significantly intensified and remained stable with little movement, forming a train effect, and resulting in continuous short-term heavy precipitation; at an elevation angle of 0.5°, the intensity of the echo center reached 58 dBZ, and correlation coefficient (CC) was nearly 1, ZDR was 3 – 4 dB, and KDP was approximately 3.1°/km; the echoes presented a low-center and high-efficiency structure, which were echo characteristics of the typical warm-sector rainstorm (Fig.3).

2.3.2 Satellite monitoring characteristics. The FY-4B satellite monitoring reveals that from 09:00 to 10:00 on June 13, the convective cloud cluster in northern Fujian continued to develop and merge; the brightness temperature on the top of clouds was low, and the top of clouds was high; the convection developed vigorously, and the cloud cluster moved slowly, which highly corresponded to the falling area of the rainstorm on the ground.

2.3.3 Ground-based dense observation. At stations such as Kaishan Township in Taining and Bailian Town in Jiangle (Fig.4), 5-minute, 1-hour and 3-hour rainfall continuously exceeded the thresholds, and short-term rainfall increased rapidly, providing direct real-time evidence for disaster warning and calling for evacuation.

3 Verification and application evaluation of numerical model forecast

Based on the verification results of the numerical models for the continuous heavy rainfall process in Sanming City from June 8 to 18, the performance of the models for the extreme rainstorm on June 13 was evaluated (Fig.5).

3.1 Global models The main rain belts of global models such as ECMWF, CMA-GFS, JMA-GSM, and NCEP-GFS were generally located to the east and north. There were significant deviations in the prediction of areas and magnitudes of extreme precipitation in the north of Sanming, and the models failed to accurately predict the centers of extreme rainstorms in Taining and Jiangle.

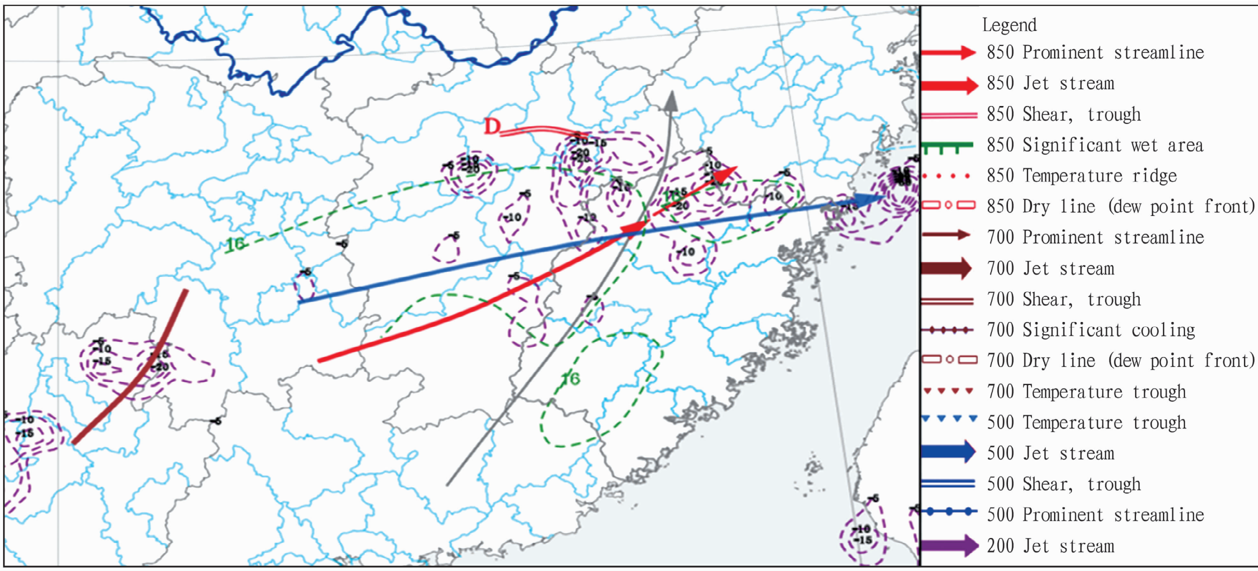

Fig. 1 Mesoscale weather chart at 05:00 on June 13, 2024

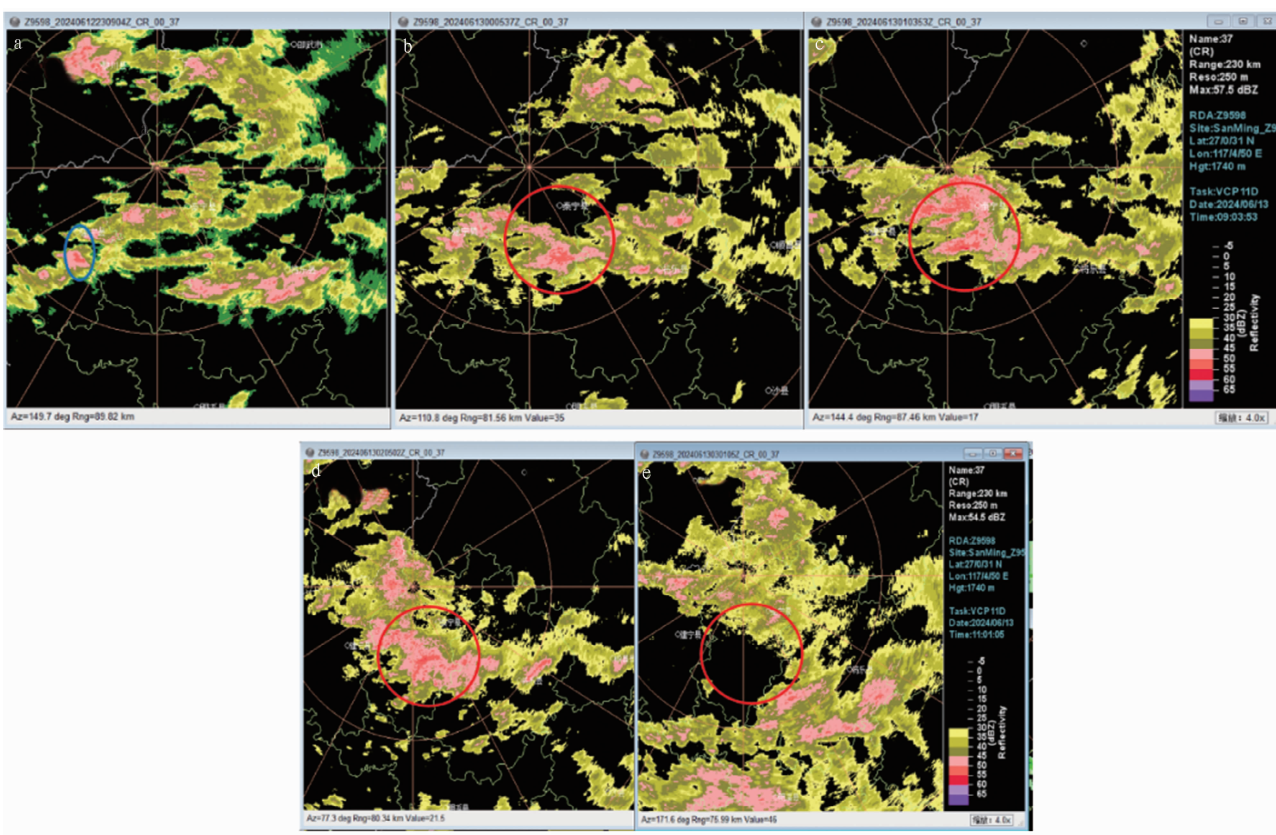

NOTE a. 07:05; b. 08:05; c. 09:05; d. 10:05; f. 11:05.

Fig. 2 Evolution of the combined radar reflectivity in Sanming City from 07:00 to 11:00 on June 13, 2024

3.2 Regional models The predicted positions of rain belts based on CMA-MESO (3 km), CMA-TYM, and Fujian regional model were close to the actual positions, but their predictions for the intensity and movement speed of the echoes were relatively weak; the predicted positions of rain belts based on the East China regional rapid assimilation system were highly consistent with the actual situation, and it had a stronger ability to forecast the development and maintenance of strong echoes, which can be used as the core basis for issuing the red alert for rainstorms.

3.3 Implications of model application Global models had limited ability to forecast extreme local rainstorms, and there were often deviations in the location and magnitude; regional rapid assimilation, radar extrapolation, and other short-term forecasting products had higher value for the warnings of extreme rainstorms. In forecast services, short-term monitoring should be prioritized while short-term forecast is as a supplement, and rolling corrections and graded warnings are conducted.

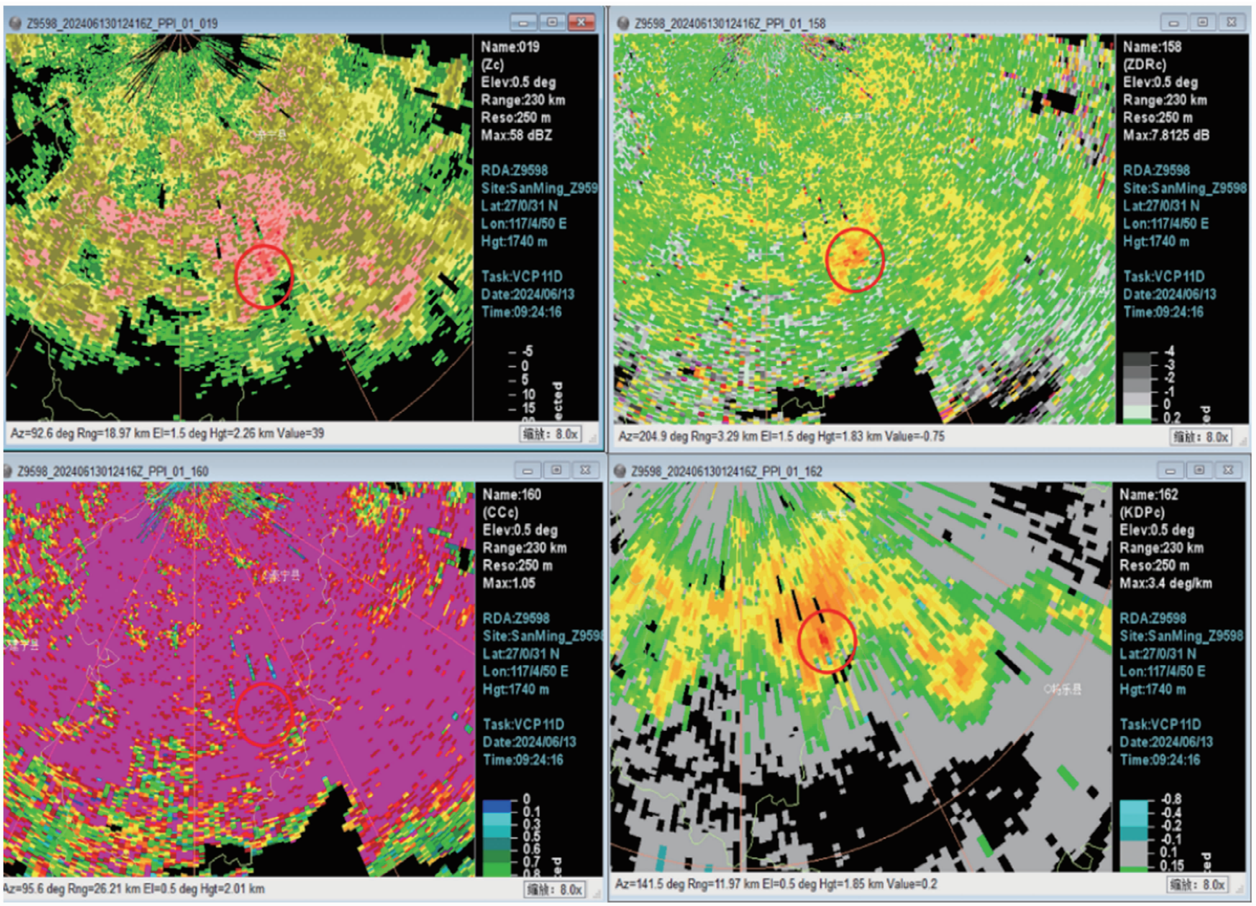

Fig. 3 Characteristic maps of Z, ZDR, CC, and KDP of a super single cell in Sanming City at 09:24 on June 13, 2024

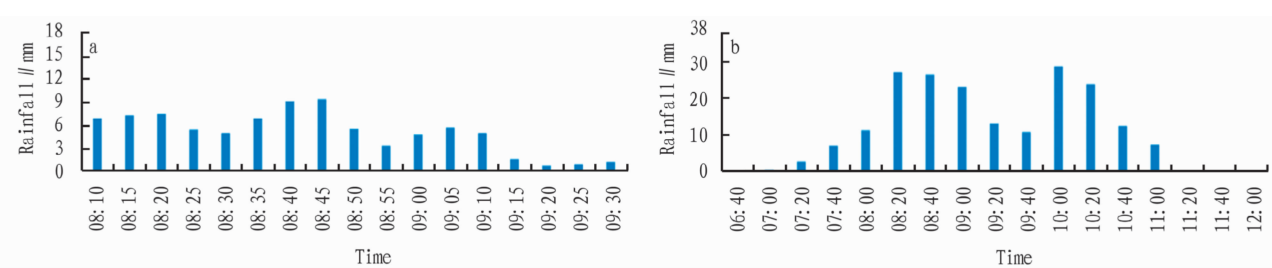

Fig. 4 5-minute (a) and 1-hour (b) rainfall in Kaishan Township in Taining on June 13, 2024

4 Summary of forecast and warning service technology

4.1 Typical characteristics of the process Based on the common features of the continuous heavy precipitation process from June 8 to 18, this extreme rainstorm on June 13 has some typical characteristics as follows: firstly, as a warm-sector rainstorm, it was triggered by the southwest jet stream, shear convergence, and deep moist layer, with no obvious intrusion of cold air; secondly, the train effect causes disasters, and the echo belts remained stable, and the same area was continuously affected by heavy precipitation; thirdly, it happened suddenly, and rainfall intensity increased rapidly, so the lead time for warning issuance was short; fourthly, due to the common effect of saturated soil caused by previous precipitation and extreme short-term heavy precipitation, the risk of mountain floods and geological disasters rose sharply.

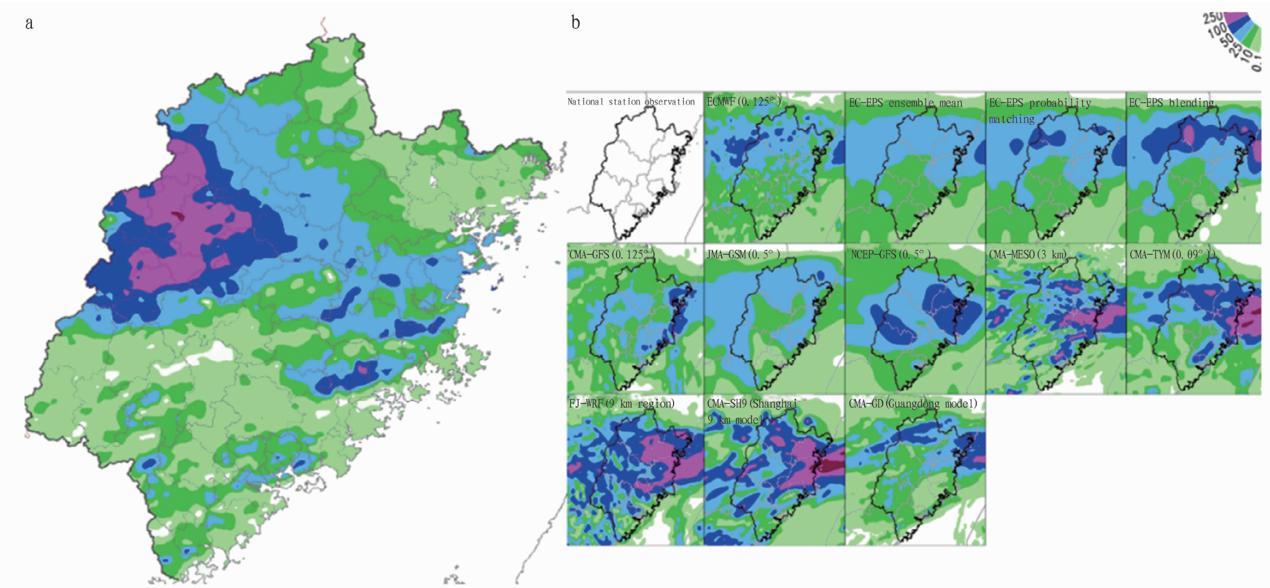

Fig. 5 **Comparison of 24-hour precipitation between the observation (a) and prediction (b) results based on different forecast models from 20:00 on June 12 to 20:00 on June 13 in 2024**

4.2 Forecast difficulty Firstly, it was difficult to make short-term forecasts for the area and magnitude of extreme precipitation, and the prediction results based on the models had systematic deviations. Secondly, the initiation and maintenance mechanisms of convection in warm-sector rainstorms were complex, and nowcasting extrapolation had great uncertainty. Thirdly, it was difficult to determine the critical threshold for the red alert standard, and there was great pressure to balance the lead time and accuracy. Fourthly, the amplification effect of local microclimate and terrain was significant, and the difficulty of making precise forecast was high.

4.3 Problems of the prediction and services Firstly, the early warnings were conservative at the initial release stage, with insufficient prediction capability for extreme rainfall; the lead time of red warnings still had room for improvement. Secondly, the monitoring scope was narrow, and it was easy to focus too much on extreme rainfall at a single point but neglect the movement and development trend of the echoes. Thirdly, there was an excessive reliance on the models and insufficient understanding of model deviations, and the subjective correction ability needs to be strengthened. Fourthly, the integration and application of multi-source observation data are not deep enough, and the supporting capacity for short-term forecast needs to be improved.

4.4 Forecast focuses In terms of the situation, the southwest jet stream, wind speed convergence, and shear line at 850 hPa should be focused on to determine the area of the rainstorm; for physical quantities, specific humidity, PWV, K index, and lifted condensation level (LCL) should be focused on to assess the potential for the warm-sector rainstorm; in terms of monitoring, radar monitoring should focus on the intensity, movement speed, centroid height, and train effect of the echoes, and satellite monitoring should pay attention to the development and movement of cloud clusters and brightness temperature; for services, regional rapid assimilation and radar extrapolation are taken as the core to make decisive classifications, issue early warnings in advance, and conduct rolling updates.

5 Comparison of precipitation processes

Based on the heavy rainfall process in Sanming City from June 8 to 18, a horizontal comparison was conducted among the towns in Nanping, Sanming, and Longyan that experienced heavy precipitation during this process. At the same time, a vertical comparison was made with the rainstorm in Taining on May 8, 2016.

5.1 Comparison of extreme precipitation in Nanping, Sanming, and Longyan Towns with more severe geological disasters during this process are taken as examples, including Kaishan Township in Taining County of Sanming, Chaping Township in Songxi County of Nanping, and Xiangdong Town in Wuping County of Longyan (Fig. 6). For Nanping (Chaping Township in Songxi County), strong rainfall was predicted daily. In fact, rainstorm to heavy rainstorm appeared, and the maximum precipitation 1 125.4 mm happened in Huangkeng Town in Jianyang County. The local government took precautions, and although there was a geological disaster and waterlogging, no casualties occurred. For Sanming (Kaishan Township in Taining County), the daily forecast values were all on the edge of heavy rainfall areas from June 9 to 13. The actual rainfall was not significant, and the prevention was relatively lax. On June 13, a sudden heavy rainstorm occurred, triggering a mountain flood, waterlogging and a geological disaster. In Longyan (Xiangdong Town in Wuping County), no strong rainfall was predicted from June 9 to 15, and the actual precipitation was not obvious. On June 16, an exceptionally heavy rainstorm occurred suddenly, and the impact of the geological disaster was relatively severe.

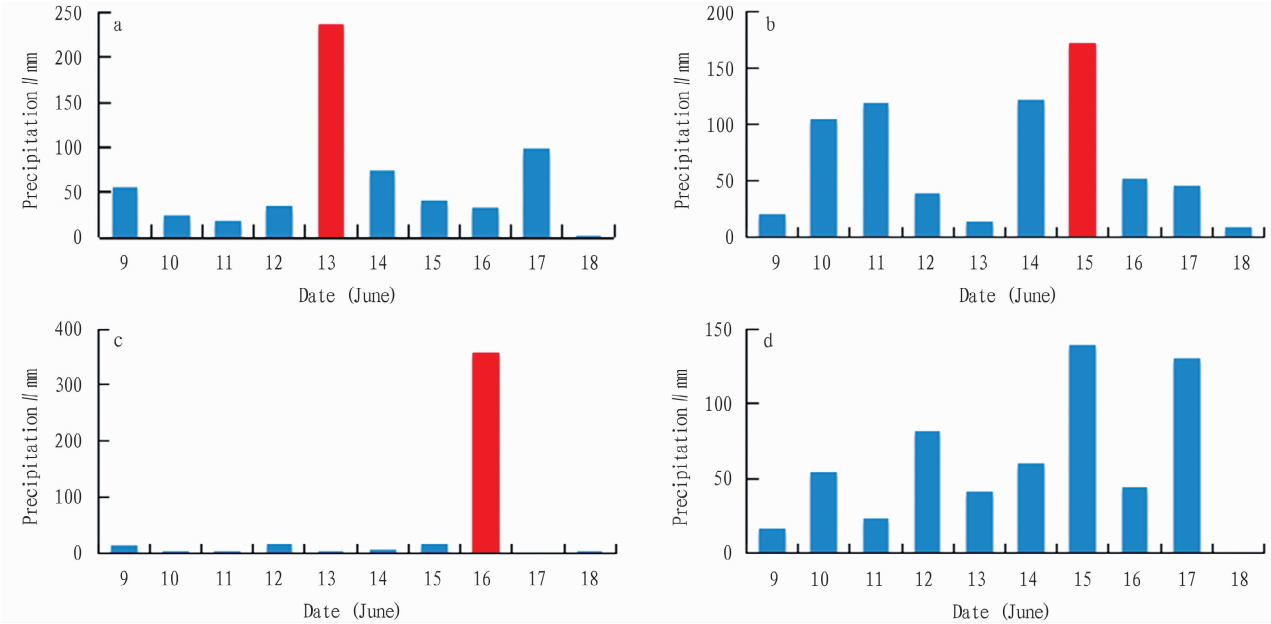

Fig. 6 Precipitation in Kaishan Township in Taining County (a), Chaping Township in Songxi County (b), Xiangdong Town in Wuping County (c), and Huangkeng Town in Jianyang County (d)

5.2 Comparison of two heavy rainfall events in Kaishan Township, Taining County From the hourly precipitation of two heavy rainfall events in Kaishan Township, Taining County on May 8, 2016 and June 13, 2024, it can be seen that the maximum hourly rainfall intensity exceeded 50 mm (Fig. 7). The comparison shows that the cumulative rainfall and 3-hour rainfall intensity on June 13, 2024 were stronger. The comprehensive intensity, duration, and cumulative rainfall on June 13, 2024 were significantly stronger than those of the event on May 8, 2016, resulting in a higher danger level of disaster-causing factors. Coupled with the previous soil saturation, the risk of mountain floods and geological disasters was higher.

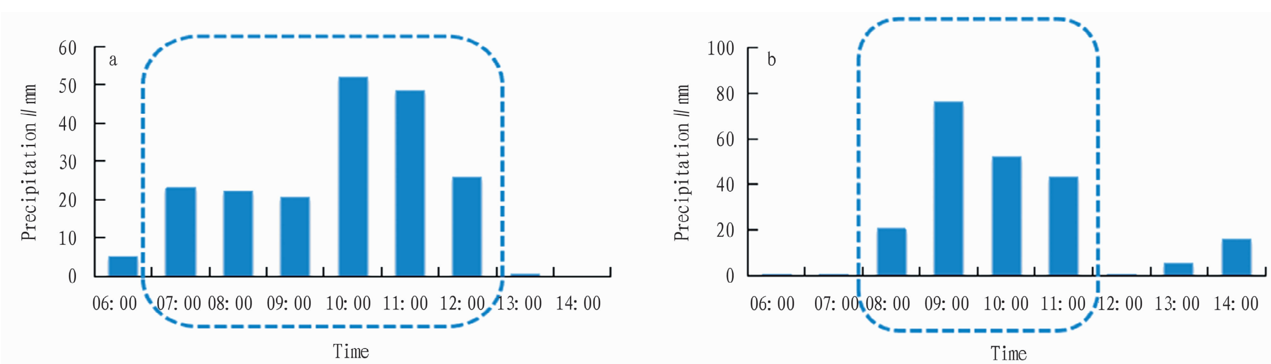

Date	Rainfall // mm				
	1 h	3 h	6 h	12 h	24 h
May 8	52.3	101.7	156.0	187.6	244.4
June 13	76.8	178.8	202.7	251.9	258.1

Fig. 7 Two heavy rainfall events in Kaishan Township, Taining County on May 8, 2016 (a) and June 13, 2024 (b)

6 Work suggestions and improvement measures

6.1 Improvement of forecasting technology Firstly, it is necessary to establish a conceptual model for warm-sector rainstorms, summarize the forecasting indicators for train-effect heavy rainstorms in the north of Sanming, and improve the criteria for terrain, jet stream, and shear configuration. Secondly, it is needed to strengthen model verification and correction, establish a deviation database for extreme heavy rainstorms, and focus on correcting the position of rain belts, echo intensity, and movement speed. Thirdly, it is necessary to promote the integration and application of multi-source data, deepen the analysis of data from ra-

(To page 48)

[2] ZHANG G, DONG J, LU L, *et al.* Acacetin exerts antitumor effects on gastric cancer by targeting EGFR[J]. Frontiers in Pharmacology, 2023, 14: 1121643.
[3] PAN BS. Research progress on myocardial injury markers and revision of diagnostic criteria for myocardial infarction[J]. Journal of Clinical Laboratory Science, 2002, 20(3): 129 – 132. (in Chinese).
[4] LI GS, YANG J, WANG Y. Effect of acacetin regulating HMGB1/RAGE signaling pathway on cardiomyocyte pyroptosis in rats with myocardial ischemia-reperfusion injury[J]. Anhui Medical Journal, 2026, 47(3): 269 – 275. (in Chinese).
[5] HAO YH, JIA YQ, ZHANG ZG. Acacetin regulates GAS6/Axl signaling pathway to alleviate myocardial injury in rats with chronic heart failure [J]. Modern Drugs & Clinical Applications, 2025, 40(10): 2420 – 2425. (in Chinese).
[6] ZHANG YM, DUAN FL. Research progress and clinical status of alcohol-related liver disease[J]. Journal of Gastroenterology and Hepatology, 1996, 5(3): 18. (in Chinese).
[7] LIU JB, WANG YH, ZHANG WW. Protective effect of acacetin on alcohol-induced liver injury in mice[J]. Journal of Higher Normal Colleges (Science Edition), 2026, 46(2): 51 – 56. (in Chinese).
[8] JI JL, ZHANG HF. Analysis of somatic symptoms of depression and related factors[J]. Chinese Mental Health Journal, 2002, 16(9): 4. (in Chinese).
[9] LI Z, MENG XY, ZHANG JH, *et al.* Therapeutic effect of acacetin on depressive rats[J]. Modern Immunology, 2025, 45(5): 555 – 561. (in Chinese).
[10] LOU SQ. Pathology and etiological factors of osteoarthritis[J]. Chinese Journal of Orthopaedics, 1996, (1): 56 – 59. (in Chinese).
[11] QIN K, WAN L, LIU J. Effect of acacetin on chondrocyte differentiation in rats with osteoarthritis[J]. Chinese Journal of Osteoporosis, 2025, 31(5): 625 – 630. (in Chinese).
[12] NIU YF, LIU MT, RONG WS, *et al.* Advances in the Pathogenesis and Traditional Chinese Medicine Intervention of Acute Lung Injury[J]. China Drug Alert, 2026, 23(6): 714 – 719. (in Chinese).
[13] CHU YJ, LIU X, LI QQ, *et al.* Study on acacetin improving acute lung injury by inhibiting NLRP3 inflammasome and cell pyroptosis[J]. Drug Evaluation Research, 2025, 48(4): 800 – 808. (in Chinese).
[14] ZHAO TJ. Vascular endothelial dysfunction and its treatment progress [J]. Foreign Medicine: Cardiovascular Disease Section, 1999. (in Chinese).
[15] ZHANG Z. Study on the mechanism of acacetin alleviating endothelial dysfunction in diabetic vascular complications[D]. Anhui University of Chinese Medicine, 2025. (in Chinese).

(From page 36)
dar, satellites, denser automatic stations, GNSS/MET, *etc.*, and improve the accuracy of short-term forecasting. Fourthly, research on terrain and precipitation should be strengthened, and research on the mechanism of terrain amplification for areas with high incidence of rainstorms such as Taining and Jiangle should be conducted.

6.2 Optimization of early warning services Firstly, the issuance of early warnings should be more decisive. Priority is given to rainfall approaching the warning threshold, and high-level warnings are boldly issued to increase the lead time. Secondly, the monitoring scope should be more comprehensive. The movement, development, and merging trends of echoes are tracked, and the affected areas are judged in advance, without being limited to rainfall at a single point. Thirdly, the call response mechanism should form a closed loop, and the full process of "release – tracking – feedback – evaluation" should be improved to ensure that the warnings reach each responsible person directly and the risk warnings reach each household. Fourthly, service products should be more refined. Integrated products including hourly rainfall, risk level, and defense suggestions are produced to enhance the decision-making support capability.

7 Conclusions

The extreme rainstorm in Sanming City on June 13 was the most extreme warm-sector rainstorm event during the continuous heavy precipitation from June 8 to 18 in 2024. It was caused by the interaction of shear lines, southwest jet stream, a deep moist layer, train effect, and topographic amplification. It was characterized by strong rainfall intensity, concentrated rainfall, local extremity, and high disaster-causing potential.

The overall forecast service for this process was effective, and the warnings were timely. Relying on radar, satellites, and regional rapid assimilation products, short-term warnings precisely supported personnel evacuation and emergency response, minimizing disaster losses to the greatest extent. However, there are still deficiencies in short-term forecast deviation, lead time of early warnings, monitoring scope, and model correction.

In the future, it is necessary to deepen research on the mechanism of warm-sector rainstorms, strengthen the integration and application of multiple sources of data, optimize warning services, improve the departmental linkage mechanism, comprehensively enhance the ability to forecast extreme heavy precipitation and provide meteorological support services, and offer more solid support for disaster prevention and mitigation in Sanming City.

References

[1] WU NG, WEN ZP, DENG WJ, *et al.* Advances in warm-sector heavy rainfall during the first rainy season in South China[J]. Journal of the Meteorological Sciences, 2020, 40(5): 605 – 616. (in Chinese).
[2] ZHANG HM, ZHANG SS, LIAN CF. Analysis of dual polarization weather radar characteristics during a heavy rainstorm in southwest Fujian [J]. Meteorological and Environmental Sciences, 2021, 44(2): 16 – 24. (in Chinese).
[3] HUANG DJ, XU XH, YE GF. Characteristics of warm-sector rainstorms in northern Fujian influenced by the Wuyi Mountains' terrain[J]. Guangdong Meteorology, 2025, 47(5): 71 – 76. (in Chinese).
[4] YIN SC, LIN RM, PEI CC. Convective characteristics and water vapor transport characteristics of a warm-sector rainstorm in Quanzhou[J]. Straits Science, 2025(10): 5 – 11. (in Chinese).
[5] DONG QR, WANG Y, LI YH, *et al.* Causes analysis of an extreme warm-sector rainstorm in Beijing – Tianjin – Hebei region[J]. Journal of Arid Meteorology, 2026, 44(1): 115 – 125. (in Chinese).